DOI:
10.1002/anie.201808613

Document Version
Peer reviewed version

Formation of Hypoxanthine Tetrad by Reaction with Sodium Chloride: From Planar to Stereo

Chong Chen[1,#], Pengcheng Ding[2,#], Manuela Mura[3], Ye Sun[2], Lev N. Kantorovich[4], Henkjan Gersen[5], Flemming Besenbacher[6], and Miao Yu[1,]*

[1]State Key Laboratory of Urban Water Resource and Environment, School of Chemistry and Chemical Engineering, Harbin Institute of Technology, Harbin 150001, China

[2]Condensed Matter Science and Technology Institute, Harbin Institute of Technology, Harbin 150001, China

[3] School of Mathematics and Physics, University of Lincoln, Brayford Pool LN6 7TS, U.K.

[4] Department of Physics, King's College London, The Strand, London WC2R 2LS, U.K.

[5] H. H. Wills Physics Laboratory, University of Bristol, Bristol BS8 1TL, U. K.

[6] iNANO and Department of Physics and Astronomy, Aarhus University, Aarhus 8000, Denmark

Emails: miaoyu_che@hit.edu.cn

[#] These authors contributed equally to this work.

Keywords: hypoxanthine, tetrad, non-planarity, ionic bonding, scanning tunneling microscopy.

Abstract

By reaction with NaCl on Au(111), the formation of hypoxanthine (HX) tetrads has been demonstrated at atomic scale in real space. At variance with guanine- and xanthine-tetrad that adopt a planar configuration with four molecules inter-linked by double hydrogen bonding (HB), the results reveal that alternative tetrads can be formed by a single-HB bonded purine in both planar and non-planar configuration. Ionic bonding plays a crucial role for the formation and planar-to-stereo transition of the HX-tetrads. Both the tilted HXs and Na show strong charge transfer with the substrate in the non-planar phase. This work provides deeper insight for constructing artificial DNA/RNA quadruplexes, and also opens up a fresh route to trigger the charge-transfer reaction of originally physisorbed molecules with a substrate as inert as Au and tune electrostatic nature of metal–organic interfaces.

Being one of the milestones of biomolecular science, the discovery of DNA/RNA quadruplex structures has inspired unceasing enthusiasm, thanks to the primary significance of quadruplexes on genome regulation as well as the considerable potentials for antitumor drug design.[1–5] Although the only quadruplex structures confirmed in human cells are guanine (G)-quadruplexes comprising stacked G-tetrads with intercalating Na^+ or K^+ cations,[6,7] enormous efforts have been devoted to exploring alternative tetrads that can potentially replace or incorporate with G-tetrads, towards applications ranging from biomedicine to supramolecular chemistry and nanotechnology.[8–10] In our recent work, stable tetrameric unit of xanthine (X) has been reported as the first alternative tetrad directly demonstrated at the atomic scale.[11] Unlike G-tetrad, where the participation of metal atoms/ions is indispensible, X-tetrad can be formed without involving any metal. G- and X-tetrads also share common features, *i.e.* adopting a planar configuration with four molecules inter-linked by double hydrogen bonding (HB). An intriguing question can then be raised: would a double HB or/and the planar configuration be indispensable for the formation of purine tetrads?

Hypoxanthine ($C_5H_4N_4O$, HX) is a primary intermediate in purine nucleotide biosynthesis that can be generated *in vivo* by deamination of adenine and oxidized to be X and uric acid *via* X-oxidase catalysis. As an analog of G lacking the amino group, HX was believed to be able to substitute G.[12,13] Since 1950's, extensive experimental and theoretical studies have been carried out to explore the tetrameric structure of HX.[14–20] Interestingly, the HX tetramer was originally recognized as a planar macrocycle,[15] but the later high-resolution (1.4 Å) crystal study proposed a bowl-like form instead.[21] Based on the reported diffraction/spectroscopic results lacking real-space observation, the structural nature of the HX-tetrad remains speculative.

Exploring the assembly of nucleobases on Au(111) in ultrahigh vacuum (UHV) has been regarded as an appropriate platform to unravel their pairing, recognition, stability and phase transitions, where the

rather weak nucleobase-substrate interaction allows for the molecular formation to be dominantly determined by intermolecular interaction(s).[22] So far, for all nucleobases and their derivatives ever reported on Au(111), the molecules were adsorbed in a flat geometry.[23-25] The *van der Waals* interactionwith Au(111), favoring planar geometry, has essentially excluded the feasibility to construct three-dimensional (3D) architectures with nucleobases "lean-on"/"standing-up" on the surface. However, stereo formations with higher diversity and complexity are certainly more desirable for understanding the nature of nucleobases in biosynthesis and physiological processes, and more preferred for advancing the synthesis of metal-organic interfaces.

Herein, we report the reaction of HX and sodium chloride (NaCl) on Au(111), by a combination of high-resolution scanning tunneling microscopy (STM) in UHV and density functional theory (DFT) calculations. It is found that HX alone cannot form HX-tetrads. However, when reacting with NaCl, typical HX tetrads are demonstrated in real space for the first time. Intriguingly, structural transformation from a planar tetrad to a non-planar form has been visualized upon increased Na/HX ratio (Scheme 1). The planar tetrad adopts a typical '*Windmill*' shape, with HXs absorbed flatly and a single Na in the tetrad center. The latter appears as a convex '*Cross*', with all HX tilted on the surface and Na deviated from the tetrad center. Single HB and Na-O ionic bonding are involved in both tetrads. At variance with the inter-tetrad double HB for the planar phase, strong Na-N ionic bonding links the non-planar tetrads into an extended network. Interestingly, due to the tilting of HX, an evident charge transfer reaction with the Au substrate occurs for both HX and Na, which not only generates two opposite dipole moments, but also strengthens the formation. These results directly demonstrate that alternative purine tetrads can be formed by a single-HB bonded nucleobase in both planar and non-planar configuration, and ionic bonding plays a crucial role for the formation and planar-to-stereo transition of the tetrads. Meanwhile, this work has opened up a fresh route to tune the electrostatic nature of metal–organic interfaces and design stereo-nanostructures on surfaces.

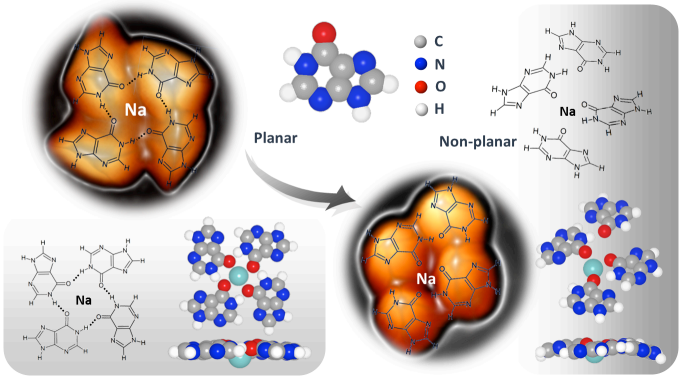

Scheme 1. Illustration of a HX tetrad and its formation on Au(111) under ultrahigh vacuum conditions.

RESULTS AND DISCUSSION

When depositing alone on Au(111), HX molecules form a disordered structure at room temperature [Details in Supporting Information (SI), Figure S1]. After a post-annealing at 400 K, two dimensional (2D) well-ordered islands are obtained (Figure 1a), with each HX appearing as a quasi-triangular motif. The HXs are packed in a highly compact manner, with the most close-packed directions slightly deviated from [1-10] and [11-2] of Au(111). Upon increasing annealing temperature until full desorption, this ordered structural phase remains the only one, indicating that no tetrameric structure can be formed by HX alone on Au(111), which is very similar to G.[11]

HX is a typical prochiral molecule that is achiral in the gas phase but becomes chiral when adsorbing on surfaces in either “face-up” or “face-down” geometry into two enantiomers (Figure 1b). Density functional theory (DFT) calculations reveal that the 2-D domains are packed side-by-side by ribbons composed of HX (Figure 1c–1d). In each ribbon, all molecules are in the same handedness, and are stabilized alternatively by intermolecular double N-H···O and N-H···N HB. Interestingly, although the individual ribbons are homochiral, the 2-D domains are heterochiral where the neighbouring ribbons are in different chirality (the L- and D-ribbons composed of L- and D-chiral HXs are marked in purple and blue, respectively, in Figure 1d). HXs in these ribbons are adsorbed flat on Au(111) at a vertical

height of 3.4 Å, showing no charge transfer with the substrate (Figure S2). The clear corrugation (Figure S3) associated with the herringbone reconstruction of pristine Au(111) visible in the image further confirms the weak HX-Au interaction.

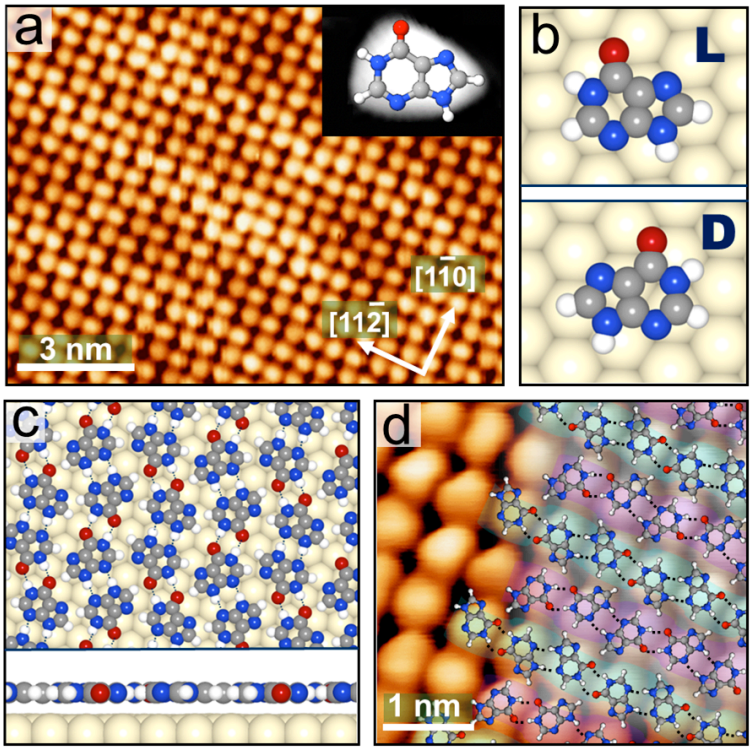

Figure 1. (a) STM image of a well-ordered 2-D molecular domain of HX, where each bright triangular protrusion is attributed to an individual HX (as depicted in the inset). (b) Adsorption-induced enantiomers, *i.e.* left-handed (L-chiral) and right-handed (D-chiral) HX. (c) Top- and side-views of the DFT structural model of HX self-assembled on Au(111). (d) High resolution STM image with the calculated structural model superimposed.

It has been well addressed that NaCl can react with organic molecules by providing Na in the resultant organic-metal complexes.[26-28] When co-depositing HX with NaCl on Au(111), an extended well-defined network is fabricated at ~ 360 K (Figure 2a–2b). The porous network is interconnected by square HX tetramers as building blocks, which appear in a typical '*Windmill*' conformation. The building blocks joint with four neighboring tetrads in a square symmetry, with the unit cell parameters of a = 2.1 ± 0.1nm, b = 2.0 ± 0.1 nm (Figure 2a). The edges of the networks are always terminated by the tetrads, confirming the tetrads as stable individual entities serving as bricks from which the entire

network is built (Figure S4). Consistent with the previously observed complexes of G and Na,[11] Na is invisible in most STM images, only showing contrast as a circular lobe at the tetrad center at a specific tip state (Figure 2c).

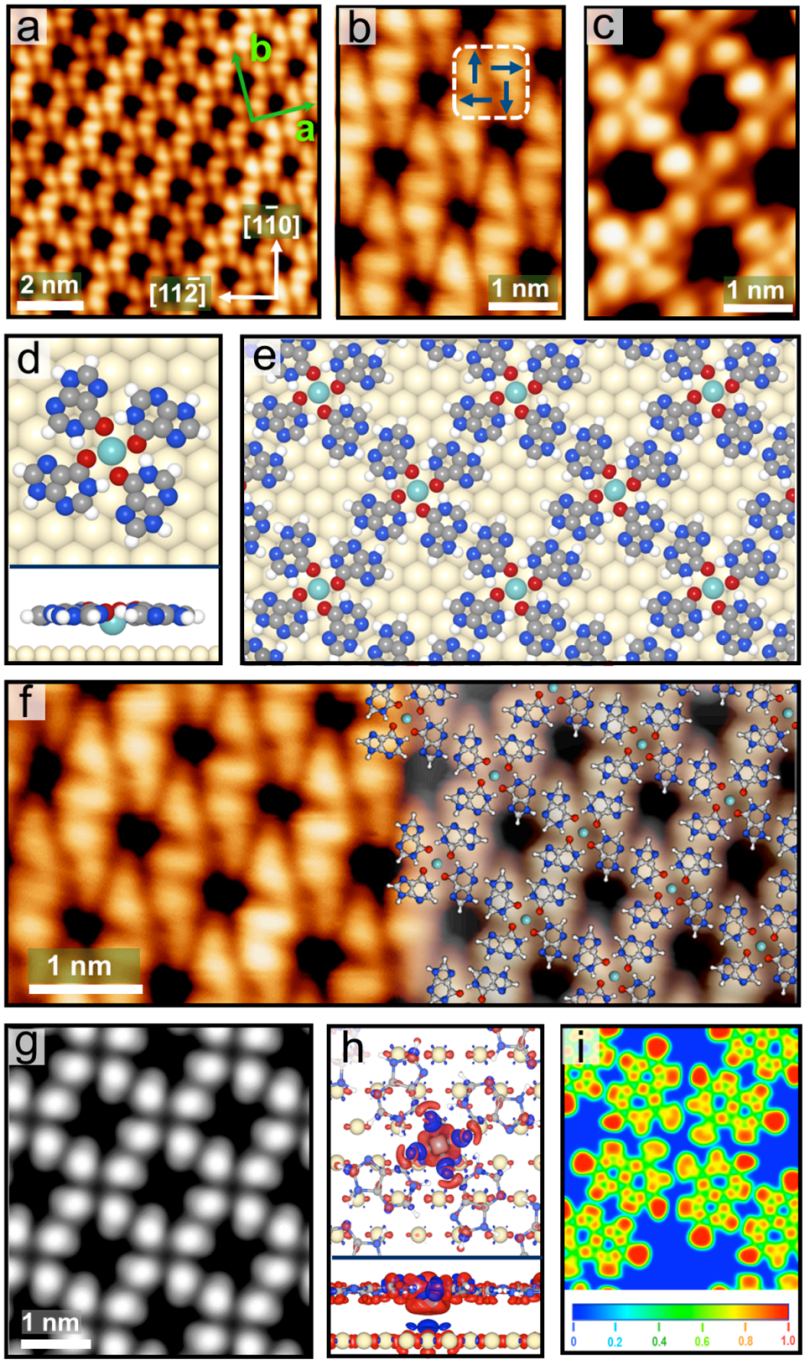

Figure 2. (a) Large-scale STM image of the open network of planar HX tetrad−Na, which is interconnected by windmill-like units. (b-c) Close observation of the HX tetrad-Na network, with either invisible Na (b) or visible Na (c) in the tetrad center, which may be attributed to the tip state. The clock-wise rotation of HXs within the tetrads is depicted

by the arrows in panel b. (d) Top- and side-view of a single planar HX tetrad-Na unit on Au(111) modeled by DFT, revealing a configuration allowing both single N-H···O HB between neighboring HXs and Na-O ionic bonding. (e) DFT calculated model of the planar HX tetrad−Na network on Au(111), where the tetrads are connected *via* inter-tetrad double N-H···N HB. (f) High-resolution STM image with the DFT relaxed structure superimposed. (g) Simulated STM image, (h) Top- and side-view plots of the charge density difference, and (i) mapping of electron localization function (ELF) of this planar HX tetrad-Na network on Au(111). In panel h, the isosurface value is 0.01 e $Å^{-3}$, where red and blue colors indicate charge depletion and accumulation, respectively.

Based on the DFT calculations, the HXs in the tetrad remain flat on the surface at an identical adsorption height of 3.4 Å, which is the same as for the case of HX alone described above. Each unit consists of four HXs (*i.e.* a tetrad) with one Na. Within the tetrad, the planar HXs interact with neighboring molecules by a single N−H···O HB (Figure 2d), consistent with the earlier structural model of a planar HX-tetrad.[19] The Na atom locates in the central point of the square defined by the four O atoms of HX. The tetrads are then further developed into the extended network by inter-tetrad double N-H···N HB (Figure 2e). Both geometry and morphology of the modeling results are in good agreement with the experimental observations (Figure 2f–2g). Na adopts a vertical height of 2.8 Å (Figure 2d and 2h), which is by 0.4 Å higher than the height of Na being alone on Au(111). In this case, no charge transfer between HX and the substrate is visible (Figure 2h); the Na-Au charge transfer is negligible. The distance of Na to the four O atoms is rather small (2.3 Å), enabling strong electron transfer between Na and O. We then profiled the electron localization function (ELF) to provide an intuitive mapping of electron localization within the network,[29-32] further confirming the Na-O ionic bonding. Na is positively charged (+0.82 *e*), hence devoting +0.21 *e* to each O atom. The increased accumulation of electrons on O enhances the strength of a single N−H···O HB to be -0.63 eV. The total ionic bonding between the Na cation and the four O atoms is calculated to be -1.99 eV. The neighboring tetrads interact *via* double N-H···N HB (-0.41 eV/bond). The overall interaction energy for each planar HX tetrad-Na unit, including (1) the adsorption of HX and Na on Au(111) (-6.49 eV), (2) the contribution of

the ionic bonding, and (3) the inner- and inter-tetrad HB, is deduced to be -11.56 eV, *i.e.* -2.89 eV associated with each HX.

It is noticed that the four HXs in each tetrad are in the same handedness, comprised exclusively of D-chiral HXs. The tetrad shows conformational chirality, where the four HXs are rotated by 90° one after another clockwise and hence surrounding the Na into a typical mononuclear windmill structure, as depicted by the arrows in Figure 2b. Not only the tetrad itself, the extended tetrad network is also homochiral, tiled by the same tetrads. Interestingly, counter-clockwise windmill units are also observed (Figure S5), where each tetrad in the network is composed of four L-chiral HXs instead. Statistical analysis reveals no preferential occurrence of any of the two tetrads. All 2-D networks are homochiral, *i.e.* containing exclusively tetrads with the same handedness.

At a higher annealing temperature (~410 K), the porous network is transformed into a close-packed new phase (Figure 3a). The building block unit still involves tetrameric HXs, but deformed as compared to the '*Windmill*' unit, forming a distorted-'*Cross*' configuration. High resolution STM image at a special tip state reveal that the Na in the tetrad is not located exactly in the middle of the four HXs anymore, but in the triangle center defined by the O atoms of the closest three HXs (Figure 3b). Besides the Na within each tetrad, there are additional protrusions (marked by the white dotted circles) which are attributed to additional Na atoms placed between the neighboring tetrads. Consistent with the literature, a higher annealing temperature can facilitate more Na atoms to incorporate into the purine network.[26] Moreover, a statistical evaluation based on the numbers of molecules in a given area range (200 Å × 200 Å) indicates that this structural phase is even more compact (~102%) than the close-packed assembly of pure HX on Au(111) discussed above. To accommodate so many molecules and Na per unit area, it is natural to assume that HXs are in a non-flat adsorption geometry.

To clarify the observations, DFT calculations were employed to further analyze the geometry and

stabilization energy of this structural phase. Initially setting up the molecular adlayer to be planar (Figure S6), the resultant configuration turns into a non-planar form after full DFT relaxation, with all four HXs in each tetrad leaning with one side towards Au(111) (Figure 3c), rather than lying flat, showing a raised tetrad center and lowered edges. The inclination of each HX (with respect to the flat geometry) is different, *i.e.* 7.7°, 9.1°, 10.6°, and 10.0° for HX-*A, B, C* and *D*, respectively (Figure 3d). The Na inside the tetrad is 3.0 Å away from the surface. The Na-O distance for HX *A, B,* and *C* is 2.3 Å, 2.3 Å, and 2.2 Å. Besides this central Na (denoted as 'Na_O'), four other Na atoms surround each tetrad (denoted as 'Na_N'). All Na_N have the same height (2.7 Å), which is evidently lower than that of Na_O. In this phase, each unit cell consists of four HXs and two Na, with the cell dimensions of a = 1.53 nm, b = 1.33 nm, and the angle of 90° between them (Figure 3d). The geometry and morphology of the proposed model are both in good agreement with the experimental results (Figure 3b and 3e).

For this non-planar form, within each tetrad, there are only two single N−H···O HB (Figure 3d). Na_O evidently transfer charge to HX *A, B* and *C*, but not to *D* (Figure 3f). Unlike Na_O which is associated with the O atoms of HXs, Na_N located between tetrads demonstrates a pronounced charge transfer with the two N atoms of the neighboring HXs. The tilting of HXs and deformation of the tetrads can be attributed to the presence of Na_N, and the Na_N-N interaction pulls *D* to be close to *A* in the neighboring tetrad. Meanwhile, Na_O is shifted to the center of HX *A*, *B* and *C*. The calculated ELF mapping (Figure 3g) provides further evidence of the Na_O-O and Na_N-N ionic bonding, which interaction energies are calculated to be -2.27 eV and -0.74 eV per unit, respectively. The charges of Na_O and Na_N in the gas phase are found to be +0.86 *e* and +0.48 *e*, respectively. When Au(111) is included, the charge on both Na is +0.84 *e*. These results indicate a significant Na_N-Au charge-transfer reaction. Moreover, due to the tilting of HXs, strong HX-Au charge transfer is also revealed. In this context, the charged HX and their image charges in Au generate a dipole moment perpendicular to the surface, while Na_N induces a dipole in the opposite direction to stabilize the structural phase by suppressing the repulsion between

HX-Au dipoles. Correspondingly, the charge transfer enhanced the adsorption of both HX and Na_N (-9.19 eV/unit). Considering all involved interactions, including (1) the ionic bonding, (2) HB, (3) dipole-dipole, and (4) adsorbates-substrate interaction, the overall interaction for each non-planar unit is -13.36 eV, *i.e.* -3.34 eV associated with each HX, indicating its higher stability than in the planar phase (-2.89 eV/molecule).

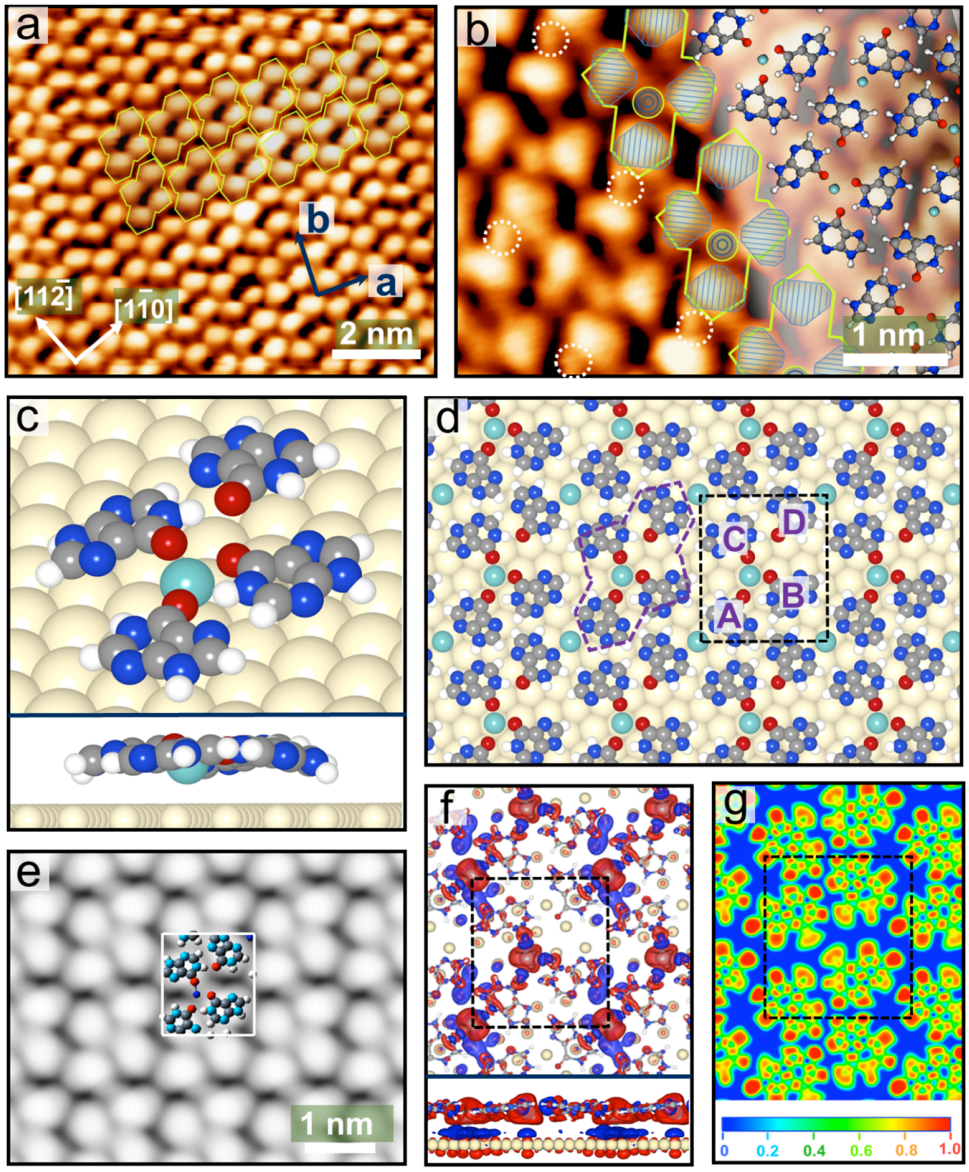

Figure 3. (a) Large-scale and (b) close-view of the close-packed HX-Na domain tiled by the '*Cross*'-shaped tetrads. In panel b, the protrusions corresponding to Na are marked by the circles. (c) Top- and side-view DFT model of a single non-planar HX tetrad-Na unit. (d) The DFT calculated model (with the unit cell shown by the dashed black box), (e)

simulated STM image, (f) plot of the charge density difference (top and side views), and (g) ELF mapping of the non-planar HX tetrad−Na phase on Au(111).

In summary, we have explored the reaction of HX and NaCl on Au(111) and visualized the typical HX-tetrads at atomic scale in real space. It is revealed that the fabrication of HX-tetrads relies on the presence of Na cations. This circumstance is unlike X, but similar to G. Surprisingly, the planar HX-tetrad is consistent with the originally proposed HX-tetrad model based on the spectral analysis,[15] not the bowl-like configuration proposed by the crystal studies.[21] With increased ratio of Na, a non-planar tetrad is indeed formed; nevertheless, its detailed structure is still distinct from the bowl model. Our results indicate that neither double HB nor planarity is necessary for the formation of purine tetrads, providing deeper insight for constructing artificial quadruplexes towards the fascinating gene regulation and anticancer strategies.

Different from the planar phase where the adlayer of HX and Na show no charge transfer with Au(111) and neighboring tetrads are connected by double HB, the non-planar tetrads are linked dominantly by ionic bonding, and both inter-tetrad Na and the tilted HXs provide strong charge transfer with the substrate. Besides HB between HXs, Na-O and Na-N ionic bonding between Na and HX, Na-Au and HX-Au bonding, and dipole-dipole interaction are all found significant. The convex configuration and charge transfer of this non-planar tetrad share certain similarity to the center-lifted assembly of 7,7,8,8-tetracyanoqui-nodimethane (TCNQ) molecules with K or Cs on Ag(100) or Ag(111),[33,34] although the co-assembly of TCNQ and NaCl showed no charge transfer with Au(111).[27] Our results thus provide a fresh route to trigger the charge-transfer reaction of originally physisorbed molecules with a substrate as inert as Au, and tune electrostatic nature of metal–organic interfaces in this way.

Conflict of Interest: The authors declare no competing financial interest.

*Address correspondence to miaoyu_che@hit.edu.cn

Acknowledgement: This work is financially supported by the National Natural Science Foundation of China (21473045, 51772066), and State Key Laboratory of Urban Water Resource and Environment, Harbin Institute of Technology (2018DX04).

References and Notes

[1] M. L. Bochman, K. Paeschke, V. A. Zakian, *Nat. Rev. Genet.* **2012**, *13*, 770–780.

[2] J. T. Davis, *Angew. Chem. Int. Ed.* **2004**, *43*, 668–698.

[3] S. Balasubramanian, L. H. Hurley, S. Neidle, *Nat. Rev. Drug Discov.* **2011**, *10*, 261–275.

[4] R. H. Hertsch, M. D. Antonio, S. Balasubramanian, *Nat. Rev. Mol. Cell Bio.* **2017**, *18*, 279–284.

[5] J. U. Guo, D. P. Bartel, *Science* **2016**, *353*, 5371–5378.

[6] G. Biffi, D. Tannahill, J. Mccafferty, S. Balasubramanian, *Nat. Chem.* **2013**, *5*, 182–186.

[7] G.N. Parkinson, M. P. H. Lee, S. Neidle, *Nature* **2002**, *417*, 876–880.

[8] S. Xiao, J. Y. Zhang, J. Wu, R. Y. Wu, Y. Xia, K. W. Zheng, Y. H. Hao, X. Zhou, Z. Tan, *Angew. Chem. Int. Ed.* **2014**, *53*, 13110–13114.

[9] M. Kinoshita, S. Takaya, T. Shibata, H. Hemmi, Y. Yamamoto, *Chem. Lett.* **2015**, *44*, 1107–1109.

[10] V. V. Cheong, C. J. Lech, B. Heddi, A. T. Phan, *Angew. Chem. Int. Ed.* **2016**, *55*, 160–163.

[11] C. Chen, H. Q. Sang, P. C. Ding, Y. Sun, M. Mura, Y. Hu, L. N. Kantorovich, F. Besenbacher, M. Yu, *J. Am. Chem. Soc.* **2018**, *140*, 54−57.

[12] M. Hajnic, A. D. Ruiter, A. A. Polyansky, B. Zagrovic, *J. Am. Chem. Soc.* **2016**, *138*, 5519−5522.

[13] M. Saparbaev, J. Laval, *Proc. Natl. Acad. Sci. USA* **1994**, *91*, 5873−5877.

[14] A. Rich, *Biochim. Biophys. Acta* **1958**, *29*, 502−509.

[15] S. Arott, R. Chandrasekaran, C. M. Marttila, *Biochem. J.* **1974**, *141*, 537−543.

[16] M. Frańska, M. Łabędzka, *Int. J. Mass spectrom.* **2012**, *323−324*, 41−44.

[17] F. B. Howard, H. T. Miles, *Biopolymers* **1982**, *21*, 147−157.

[18] G. V. Wheeler, B. Jollès, P. Miskovsky, L. Chinsky, *J. Biomol. Struct. Dyn.* **1996**, *14*, 91−99.

[19] F. B. Howard, H. T. Miles, *Biochemistry* **1982**, *21*, 6736−6745.

[20] F. C. Meng, X. Zhao, *J. Mol. Struct. Theochem.* **2008**, *869*, 94−97.

[21] B. C. Pan, K. Shi, M. Sundaralingam, *J. Mol. Biol.* **2006**, *363*, 451−459.

[22] R. Otero, W. Xu, M. Lukas, R. E. A. Kelly, E. Lægsgaard, I. Stensgaard, J. Kjems, L. N. Kantorovich, F. Besenbacher, *Angew. Chem. Int. Ed.* **2008**, *47*, 9673−9676.

[23] R. Otero, M. Schöck, L. M. Molina, E. Lægsgaard, I. Stensgaard, B. Hammer, F. Besenbacher, *Angew. Chem. Int. Ed.* **2005**, *117*, 2310–2315.

[24] M. Yu, J. G. Wang, M. Mura, Q. Q. Meng, W.Xu, H. Gersen, E. Lægsgaard, I. Stensgaard, R. E. A. Kelly, J. Kjems, T. R. Linderoth, L. N. Kantorovich, F. Besenbacher, *ACS Nano* **2011**, *5*, 6651−6660.

[25] A. Ciesielski, M. E. Garah, S. Masiero, P. Samorì, *Small* **2016**, *12*, 83−95.

[26] C. Zhang, L. Xie, L. K. Wang, H. H. Kong, Q. G. Tan, W. Xu, *J. Am. Chem. Soc.* **2015**, *137*, 11795−11800.

[27] C. Wäckerlin, C. Iacovita, D. Chylarecka, P. Fesser, T. A. Jung, N. Ballav, *Chem. Commun.* **2011**, *47*, 9146–9148.

[28] D. Skomski, S. Abb, S. L. Tait, *J. Am. Chem. Soc.* **2012**, *134*, 14165–14171.

[29] Q. Sun, Q. Wang, J. Z. Yu, V. Kumar, Y. Kawazoe, *Phys. Rev. B* **2001**, *63*, 193408–193411.

[30] Y. Xiao, Y. Liu, N. Frederick, F. C. Zhang, *Solid State Ionics* **2017**, *307*, 26–34.

[31] S. H. Zhang, Q. Wang, Y. Kawazoe, P. Jena, *J. Am. Chem. Soc.* **2013**, *135*, 18216−18221.

[32] J. R. Debackere, M. R. Bortolus, G. J. Schrobilgen, *Angew. Chem. Int. Ed.* **2016**, *55*, 11917–11920.

[33] P. J. Blowey, L. A. Rochford, D. A. Duncan, D. A. Warr, T. L. Lee, D. P. Woodruff, G. Costantini, *Faraday Discuss.* **2017**, *204*, 97–110.

[34] N. Abdurakhmanova, A. Floris, T. C. Tseng, A. Comisso, S. Stepanow, A. De Vita, K. Kern, *Nat. Commun.* **2012**, *3*, 940–946.